Optical link budget for Low-Earth-Orbit satellite and high altitude platforms for Quantum Key Distribution Missions

Ricardo Carvalho, ricardogil.carvalho@gmail.com
Instituto Superior Técnico, Universidade de Lisboa, Av. Rovisco Pais, 1049-001 Lisboa, Portugal

***Abstract*—Quantum key distribution with satellite communications are becoming more and more important nowadays because they offer a way to transmit information between two distant parties in a secure way. With Quantum Key Distribution (QKD) it's possible to share a message between two parties using fiber networks or free-space links. Quantum communication systems use photons that are encoded in a quantum state in physical degrees of freedom. These encoded photons are then sent to distant locations. Through this mechanism of encoding and decoding, two distant parties can share a string of random bits also called secret keys, which can be used to encrypt and decrypt secret messages. Although this is a very promising and innovative technology there are still limitations and challenges that need to be overcome. QKD, with both optical fibres and terrestrial free-space links, has been a case of study for many years, however, the high losses in optical fibres (exponential with distance) does not make it a feasible technology to share secret keys over large distances. The satellite-based QKD, which offers significantly smaller optical losses, has been considered has an alternative for large distances. The losses in a satellite-based optical channel are caused mainly due to the turbulence of the atmosphere and the difficulty of pointing a laser to a platform that is constantly moving. However, a issue with this solution is that the deployment and maintenance costs of satellites are very high so there will always be a barrier between the technology and the market. Another method of exploring the free space quantum technology is by using QKD systems on High Altitude Platforms (HAPs). This technology is still very recent and there are not many studies to show the feasibility of using QKD on HAPs so the main objective of this thesis is to research and study a method or system with technical parameters while simulating results that will allow achieving a QKD between Earth and HAPs.**

***Index Terms*—LEO satellites, HAP's, QKD**

I. Introduction

Quantum key distribution is a scheme for enabling two parties, commonly referred to as Alice and Bob to share a secret key between them. This sharing of information can be done using different quantum key distribution protocols. The idea is to study different payloads from previous experiments that are fit to be implemented in a HAP (High altitutde platform), while comparing the main differences between QKD on LEO satellites and HAP's. Implementing a QKD payload on a HAP is still a very recent approach because of the immature HAPtechnology and lack of global deployment capability. However some studies with HAP's have proven to be able to continuously provide commercial services such as 4G wireless communication services to remote areas by using a network of high altitude balloons. Using HAP's instead of LEO satellites for QKD systems brings both advantages and disadvantages. Satellites have predictable trajectories compared with HAP's, that despite being static have more random movements due to wind and atmospheric conditions, which need a coarse system, for example a gimble, to adjust to this random variatons. However the smaller distances to the Earth provide much less optical attenuation and possible operation during daylight. The lower deployment and maintenance costs allow the QKD service to be accessible to a larger market. The long endurance of the HAP's allow QKD services to be delivered to certain regions continuously, unlike the unavoidable service window of the QKD on LEO satellites [1]. The limitations to this technology regarding the coverage area, pointing system, link budget and a possible payload will be addressed in this paper.

II. Coverage Area

The satellite coverage area on Earth depends mainly on the orbital parameters such as the satellite position relative to a point on the Earth surface. Ground stations can communicate with LEO satellites only when there is LOS (Line of sight). The coverage area of a satellite is an elliptical area projected on the Earth surface. The largest coverage area is achieved for the lower elevation, but in order to avoid obstacles the typical values for the elevation range from 0 to 90.

The geometry between a satellite and Earth can be seen in figure 1. The different points represent the satellite (SAT), the base station (P), the distance between the satellite and the base station (d) which depends on the elevation angle (also called slant range), the line passing through P represents the horizontal plane, T is the point on the surface of the Earth that is collinear with the line that goes from the satellite to the center of the earth. There are four variables that we have to consider: ε_0(elevation angle), α_0 (nadir angle), β_0(central angle) and d (slant range). These variables are expressed by the following equations [2]:

$$\varepsilon_0 + \alpha_0 + \beta_0 = 90 \tag{1}$$

$$d\cos\varepsilon_0 = r\sin\beta_0 \tag{2}$$

$$d\sin\alpha_0 = R_e\sin\beta_0 \tag{3}$$

With R_e being the Earth Radius.

The most important parameter will be the slant range (d) which is affected by the elevation angle. From this image and applying geometrical equations we get [2]:

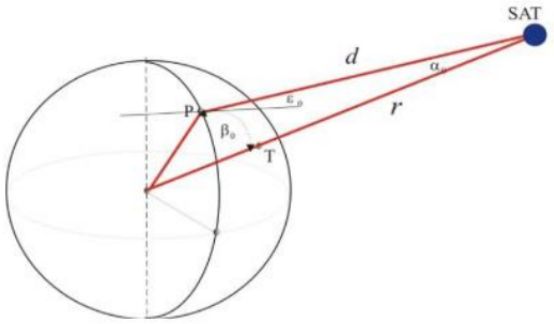

Fig. 1. Satellite and Ground Station Geometry

$$r^2 = R_e^2 + d^2 - 2R_e d\cos(90 + \varepsilon_0) \tag{4}$$

Which solved in order of d and substituting r by $r = H + R_e$, with H being the distance from the satellite to the Earth's surface in the direction of the Earth center when pointing towards the center of the Earth, different from d that is the distance from the satellite to the Earth station we get:

$$d(\varepsilon_0) = R_e \left[\sqrt{\frac{H + R_e}{R_e}^2 - \cos^2 \varepsilon_0} - \sin \varepsilon_0 \right] \tag{5}$$

By applying the sinus theorem we get the equation [2]:

$$\sin \alpha_0 = \frac{R_e}{R_e + H} \cos \varepsilon_0 \tag{6}$$

For different elevations (ε_0) we calculate α_0 and then based on equation (1) we calculate β_0 . Now knowing these parameters we are able to calculate the surface of the covered area which is described by the following equation [2]:

$$S_{coverage} = 2\pi R_e^2 (1 - \cos \beta_0) \tag{7}$$

III. Bit-Error Rate and Photodetectors

The performance of the optical receiver in a digital transmission system is measured by the Bit-Error Rate (BER). The BER is defined as the ratio between the number of received bits incorrectly detected and the total number of bits transferred in a given time interval. Usually for this kind of optical communications the values vary between 10^{-6} and 10^{-9} [3].

The photodetector is the element of the optical receiver used to convert the optical signal into an electrical signal(direct detection - DD receivers employ a photodiode as square-law device, resulting in an electrical signal proportional to the power of the incident signal, i.e the optical signal power is directly measured. There are two types of photodiodes used in optical communications, the pin photodiode and the avalanche photodiode (APD).

The APD performance is characterized by its responsivity, R_{APD}, which is the relationship between the output electric current and the optical power incident on the APD. The APD responsivity is given by:

$$R_{APD} = \frac{\eta \lambda}{1.24} \tag{8}$$

With η being the quantum efficiency of the detector.

An APD multiplies the generated primary photoelectrons by its avalanche gain M (e.g M = 100 for Si APDs and M = 10 for InGaAs APDs). This effect comes at the expense of multiplication noise. The following table presents typical photodetectors characteristics [4].

Photodetector	**Wavelength (nm)**	**Responsivity (A/W)**	**Dark Current (nA)**
Silicon PIN	550 - 850	0.41 - 0.7	1 - 5
Silicon PIN	850 - 950	0.6 - 0.8	10
InGaAs PIN	1310 - 1550	0.85	0.5 - 1.0
InGaAs APD	1310 - 1550	0.80	30
Germanium	1000 - 1500	0.70	1000

The electrical current generated by the photodetector is directly proportional to the incident optical power. However this current is not always constant and has fluctuations caused by different types of noise such as the quantum noise and the circuit noise [3]. The optical signal that is incident on the photodetector corresponds to a certain average number of photons per unit of time. The time slot between photons is random and the photocurrent generated by the photodiode is not a continuous process. The photodetector generates a small current in the absence of any optical signal. This current is called dark current, I_d, and comes from the thermally generated electron-hole pairs. This dark current also affects the quantum noise at the photodiode [3].

The quantum noise, in certain situations called shot noise, is the random fluctuations in the number of photons that reach the detector from point to point, and is given by:

$${\sigma_q}^2 = 2q(r_0 P_i + I_d) M^2 M^x B_{e,n} \tag{9}$$

Where q is the electron charge, M is the avalanche gain, x is a photodiode material parameter with values between "0" and "1" and $B_{e,n}$ is the equivalent noise bandwidth from the optical receiver.

The circuit noise depends on the temperature and resistive and active elements in the optical receiver, so its value depends on the remaining electrical elements present in the receiver, such as the amplifier.

Usually the output signal of the photodetector is very weak and needs to be amplified in order for it to be processed by the other system devices. So an electrical amplifier is used to amplify the electrical current generated by the photodetector. As mentioned before, the electrical components of the photodetector contribute to the circuit noise.

The circuit noise current variance is given by:

$$\sigma_c{}^2 = \left[\sqrt{\frac{4k_BTF_n}{R_L}}\right]^2 B_{e,n}G_A^2 \tag{10}$$

Where G_A is the amplifier gain, k_B is the Boltzmann constant, T is the absolute temperature R_L the load resistance of the photodetector and F_n is the noise factor of the amplifier.

The total noise current variance, σ_n^2, is the sum of the quantum and circuit noise variances:

$$\sigma_n^2 = \sigma_q^2 + \sigma_c^2 \tag{11}$$

IV. Pointing System

Free-Space Optics offer many advantages for systems with limitations regarding size, weight and power. To achieve this potential, one of the main limitations for LEO satellites concerning FSO communications has to do with the PAT (pointing, acquisition and tracking) system that must be very accurate since the satellite has a certain velocity and it must have the laser constantly pointing to the base station. On the other hand for HAP's, one important thing to take into consideration is that the BS is stationary and the HAP's itself is quasi-stationary so the establishment, measurement and maintenance of the links is much less demanding compared to a LEO satellite, since beam tracking and adjusting are less necessary.

Despite the tracking on HAPS being much more easier than on LEO satellites, there is still the need for a tracking system that complies with the movement of the spacecraft. This chapter will be based on NODE (Nanosatellite optical downlink experiment), which is a low-cost, commercial off the shelf (COTS) laser downlink experiment, being designed and developed at MIT [5]. NODE is approximately 1U and so is a communications payload easily applicable to numerous CubeSat's. Node uses different wavelength lasers for different purposes:

- The beacon signal is a 976 nm laser used to detect the base station.
- The downlink signal is a 1550 nm laser used to transmit data.
- The 635 nm laser is used as a feedback laser for the FSM pointing angle.

For the laser uplink tracking the most important piece of hardware is the on-board camera at the nanosatellite. The focusing lens is used to detect the incidence of the beacon laser on the detector and then determine the angle of the incident beam. The most important thing when choosing a lens is the Focal Length, which determines the field of view of the detector. The mirror is used to determine the route of the optical signal depending on the wavelength. Acts as a mirror for the 1550 nm signal (downlink) since it reflects the signal out of the main satellite aperture. Acts as a beamsplitter, partially passing and partially reflecting the beacon laser to be detected on the camera lens. Acts as a window for the 976 nm signal do that the beacon detectability is not worsened. The bandpass filter is added to the satellite main aperture to block light from earth and therefore minimize the noise on the beacon detector. The FSM (flexible steering mirror) is crucial to the pointing system as it guides the downlink beam in the direction of the ground station based on the beacon's angle of incidence. A collimator, which is a device which narrows a beam of particles or waves. Turn the optical signal propagated in the fiber into a free space beam. In the following picture drawn by the author in [5] , we can see how the tracking and pointing system works in the NODE experiment.

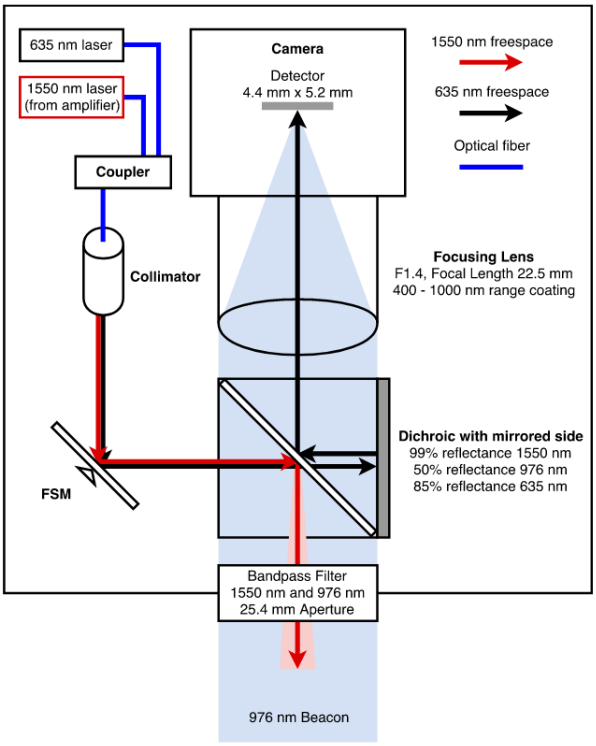

Fig. 2. Diagram of the NODE pointing and tracking system [5]

V. Link Budget Analysis

Free space optical communication links transfer information between a transmitter and a receiver using an optical carrier and a free space channel. During this transfer there are many aspects that affect the signal such as the atmospheric effects. For FSO communication, eddies in the turbulent atmospheric channel cause random variations in the intensity of the received signal. Atmospheric turbulence, the main attenuation parameter in Earth to satellite FSO, is the atmosphere temperature and pressure variations resulting in fluctuations in the atmospheric density, affecting the signal received. The issues involved in the FSO communication in laser uplink are different from the ones in the downlink for LEO satellites. For HAPs since the altitude is around 20 km the effects of the turbulence on the downlink and uplink are similar, with the PAT being the main issue. For LEO satellites in the case of laser uplink (ground to satellite) , the beam comes immediately in contact with the atmosphere and therefore suffers more from distortion and pointing instability due to changes in the

refractive index of the atmosphere. On the other hand, for laser downlink (satellite do ground), it causes the beam to spread geometrically (caused by beam divergence loss), and very little spread is due to the atmospheric effects. Due to these aspects, the effect of atmospheric turbulence is smaller on the downlink propagation compared to the uplink propagation, as the beam goes through a non-atmospheric path until it reaches about 30 km from the Earth's surface.

Quantum Key Distribution systems rely on optical communications link analysis to have enough photons arriving at the receiver. The main factors that have to be taken into consideration regarding optical communications are the distance between the transmitter and the receiver, the operating wavelength, all the losses related to the atmospheric conditions, geometrical losses, the channel turbulence, the background noise and the optical losses.

In the following study we will take a look at the different parameters that affect the channel loss on an optical link based on Pfennigbauer et al. method [6] and based on the paper by [7], where two different methods to calculate the channel losses are used and compared.

Geometrical Losses

These losses result from the natural spreading of the beam and make the beam deviate from its original path. They are given by:

$$L_{geo} = 20\log_{10}\left(\frac{D_{tx} + \frac{H_{hap}}{\sin\alpha}1.22\frac{\lambda}{D_{tx}}}{D_{rx}}\right) \tag{12}$$

Where D_{tx} is the transmitter aperture size, D_{rs} is the receiver aperture size, R_{Los} is the line of sight distance, H_{hap} is the altitude of the HAP, α is the elevation angle and θ is the beam divergence angle.

Attenuation due to Fog, Snow and Rain

This type of attenuation has to do with the visibility range of the Link. The visibility range for different weather conditions such as fog, snow and rain, according to Kim model is given by:

$$L_{fog} = \frac{3.91}{V}\left(\frac{\lambda}{550}\right)^{-p}(dB/km) \tag{13}$$

$$L_{snow} = \frac{58}{V}(dB/km) \tag{14}$$

$$L_{rain} = \frac{2.8}{V}(dB/km) \tag{15}$$

where

$$p = 1.6\ when\ V > 50$$

$$p = 1.3\ when\ 6 < V < 50$$

$$p = 0.36V + 0.34\ when\ V < 6$$

.

Where V is the visibility range (km) and p is the size distribution coefficient of scaterring.

The distance that the optical signal travels through weather is given by:

$$R_w = \frac{H_w}{\sin\alpha} \tag{16}$$

Attenuation due to the misalignment of the beam

Misalignment can occur due to the turbulence in the atmosphere, which is the constant difference in temperature and pressure along the stratosphere. This difference can cause random deflections in the beam with its centroid being randomly displaced:

$$L_{p1} = 0.54R_{Los}^2\left(\frac{\lambda}{D_{tx}}\right)\left(\frac{D_{tx}}{r0}\right)^{\frac{5}{3}} \tag{17}$$

The random movements of HAPs due to, for example, wind can cause difficulties in the pointing system, which result in attenuation given by:

$$L_{p2} = exp\left(\frac{-8{\theta_j}^2}{\theta^2}\right) \tag{18}$$

Link Budget from NanoBob

To make a comparison between some results, the author makes a comparison between different methods used to calculate the link budget. The other method is based on the "Nanobob: a Cubesat mission concept for quantum communication experiments in an uplink configuration" [8]. This method is described as:

$$L_{Nano} = \frac{L^2(\theta_T^2 + \theta_{atm}^2)}{D_R^2}\frac{1}{T_t(1-L_p)T_R}10^{\frac{A_{atm}}{10}} \tag{19}$$

Where T_R and T_T are the transmission factors of the receiver and transmitter telescopes, respectively. L_p is the pointing loss due to misalignment, and A_{atm} is the atmospheric attenuation due to Rayleigh scattering and absorption (in dB). It equals to 3 dB at 808 nm and 2 dB at 1550 nm. The beam divergence angle is given by:

$$\theta = 2.44\frac{\lambda}{D_{tx}} \tag{20}$$

And the atmosphere turbulence included divergence angle is given by:

$$\theta_{atm} = 2.1\frac{\lambda}{r0} \tag{21}$$

According to the author, the definition of θ is different from the one from Pfennigbauer et al. [5] because they dont want to underestimate the effect of atmospheric turbulence so $L.\theta_T$

corresponds to the full diameter of the central spot in the Airy diffraction pattern instead of its radius. And for the same reason the author used the original definition for eq. 3.34, despite some authors using $\theta_{atm} = \frac{\lambda}{r_0}$, without the 2.1 factor, which equals the ratio of the spatial coherence radius to the Fried parameter.

The Fried parameter, $r0$ is dependent on the turbulence strength and is given by:

$$r0 = [0.423k^2 \int_0^h C_n^2(z')\, dz']^{\frac{-3}{5}} \tag{22}$$

To calculate the turbulence strength we can use the Hufnagel-Valley Boundary (HVB) model which is commonly used for ground to satellite communication link. This model includes parameters for the atmosphere up to a height of $24km$, can be used for both day and night time and can be used at different locations since it accounts for the variations in wind velocity and on different ground turbulence conditions.

$$C_n^2(h) = 0.00594 \left(\frac{V}{27}\right)^2 (10^{-5}h)^{10} exp\left(-\frac{h}{1000}\right)$$
$$+ 2.7{\cdot}10^{-16} exp\left(-\tfrac{h}{1500}\right) + A exp\left(-\tfrac{h}{100}\right) \tag{23}$$

Usually the Fried Parameter $(r0)$ has a typical value of 10 cm to 20 cm at an optical wavelength of 500 nm. The Fried Parameter gets smaller when the turbulence is stronger and theoretically $r0$ is proportional with $\lambda^{\frac{6}{5}}$. It's safe to use values around 20 cm for these experiments.

VI. Payload

The optical payload system layout is based on the Cubesat Infrared CrosslinK mission (CLICK) which is a collaboration between the MIT, the Radiation Laboratory (STAR Lab), the Precision Space Systems Laboratory at the University of Florida and NASA Ames Research Center. This experiment aims to develop a pair of CubeSats to demonstrate a nanosatellite inter-satellite link as well as a downlink to a MIT portable optical ground station [9].

The payload optical system layout is about 1.5U and is shown in Fig. 3. There are three optical paths which are the Beacon received signal to aid on the pointing accuracy, and the communications transmitted and received signals. The objective of the fine pointing system (FPS) is to align the transmitted and received communication signals in order to accomplish the pointing requirement. The laser spot sensor is a Quadcell which consists on 4 PIN photodiode sensors. The beacon signal is detected on the quadcell and the output signals are amplified via an APD transimpedance amplifier and a bandpass filter [9].

In order to meet the low SWAP requirements of a CubeSat, the CLICK payload does not use a coarse pointing gimbal, instead relies on the ADCS of the spacecraft. On my study, the payload will be set on a HAP which is capable of higher SWAP requirements. In this type of design the optical bench

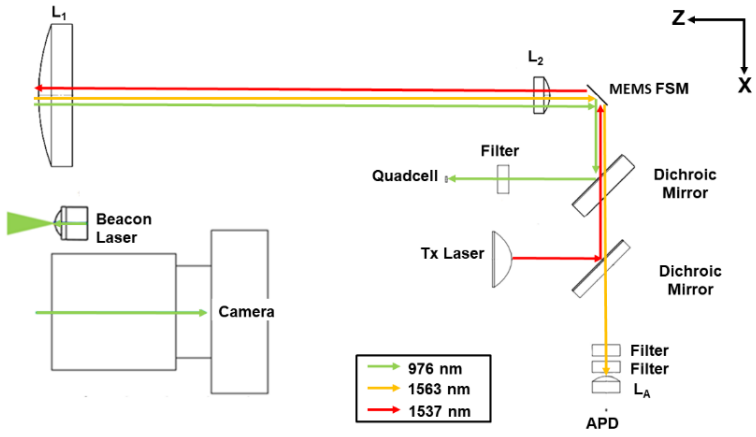

Fig. 3. CLICK Payload Optical Layout [9]

includes the fine pointing and tracking system and the gimbal will be used for coarse pointing, acquisition and tracking. The gimbal used for the experiment will be the FOXTECH SEEKER-30 TIR 30X Optical Zoom and Thermal Camera with 3-axis Gimbal depicted in Fig. 4, which has an error of 0.01.

Fig. 4. FOXTECH Gimbal for coarse pointing, acquisition and tracking

This 1.5U volume limit payload (96 × 96 × 147 mm) with a mass of $1,5kg$ can be accomodated in different ways. The selected design layout is shown in figure 5.

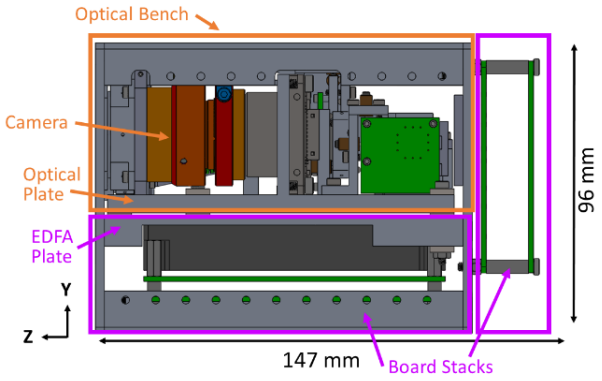

Fig. 5. Side view of the Payload (+X) [9]

The optical telescope and camera are pointing out of the +Z face. The optical components are coupled into a small volume of 95 × 56 × 119 mm). The upview of the optical components are depicted in figure 4.6.

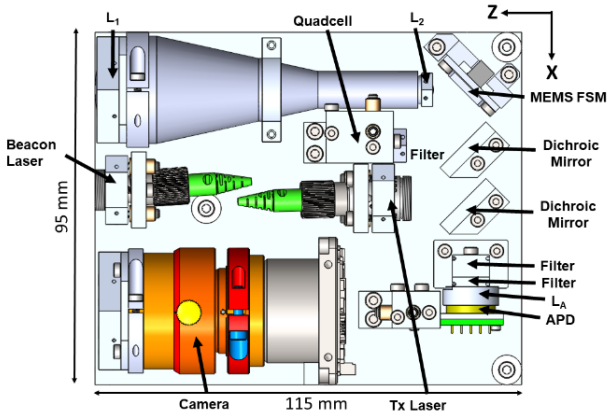

Fig. 6. Up view of the optical components [9]

VII. QKD

The BB94 Protocol is a QKD protocol proposed in 1984 by Bennet and Brassard. The objective of this protocol is to encode every bit of the secret key into the polarization state of a single photon. An attempt to measure an incoming photon in an unknown polarization state will introduce disturbance and therefore it will be possible to detect an outside attack. In the BB84 protocol, Alice sends a sequence of pulses where , ideally, each pulse contains a single photon with a certain polarization. Here, Alice sends single photons randomly polarized horizontally or vertically (straight base), or +45 or -45 (diagonal base) where The 'D' polarization corresponds to 1 and the 'A' polarization to 0.

At the receiver Bob measures the polarization state of the photons with the adequate setup, and he is able to distinguish between the H and V polarizations if he uses the HV basis. In

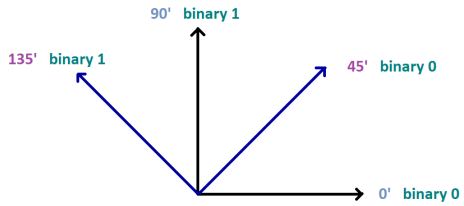

Fig. 7. Photons Polarized in 2 basis

Half of the cases Bob randomly changes his measuring basis to AD. After a certain number of bits have been transmitted, Bob announces which basis he used for each bit and compares it with Alice. Alice then says in which cases they used the same basis and they throw out the bits where they used different bases. After this procedure, called key shifting, they reduce the length of the key twice, and what is left, despite being random, coincides for Alice and Bob. After this procedure they take out a small part of the key, for example 10% and compare it to check for eavesdropping. This part of the key is made public and is later discarded. But if they see that there are errors in the key, the whole key is discarded and the procedure is repeated again [10].

E91 Protocol

The E91 Protocol was proposed in 1991 by Artur Ekert and uses entangled pairs of photons. These can be created by Alice, Bob or by some source separate from them, including the eavesdropper Eve. The photons are distributed so that Alice and Bob end up with one photon from each pair. This scheme relies on two properties of entanglement. First, the entangled states are perfectly correlated in the sense that if Alice and Bob both measure whether their particles have vertical or horizontal polarizations, they always get the same answer with 100% probability. The same is true if they both measure any other pair of complementary (orthogonal) polarizations. This needs for the two distant parties to have exact directionality synchronization. However, the particular results are completely random. It is impossible for Alice to predict if she (and thus Bob) will get vertical polarization or horizontal polarization. Second, any attempt at eavesdropping by Eve destroys these correlations in a way that Alice and Bob can detect [10].

cm

B92 Protocol

The B92 protocol was proposed in 1992 by Bennet and uses two non-orthogonal states, for instance H for 0 and D for 1.

Alice sends 0's in the HV basis and 1's in the AD basis. Bob chooses the basis randomly, if he gets V polarization in the HV basis, it means it can't be H so he writes down '1'. But if , on this basis he gets a H, it can also be a D, so the result is inconclusive and this bit is discarded (Figure 3.3).

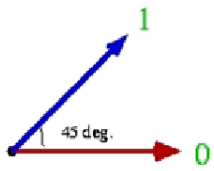

Fig. 8. Two non orthogonal states, H for 0, D for 1

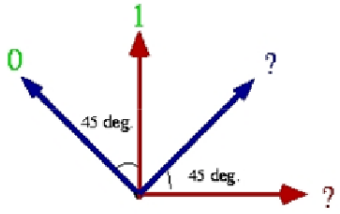

Fig. 9. Possible results for Bob

The same if Bob uses the DA basis and obtains D, it could be D but could also be H, so the result is again inconclusive. Only if Bob gets an A in the AD basis he writes '0' because it could not be D. The B92 can also be applied to continuous-variable states but is believed to be less secure than the BB84 protocol [10].

VIII. Photon Sources

A variety of of techniques have been proposed for QKD. QKD protocols can be divided into two categories: discrete variable QKD (DV-QKD) or continuous variable QKD (CV-QKD). In DV-QKD information is encoded onto discrete degrees of freedom of optical signals. In CV-QKD, information is encoded into the quadratures of randomly selected coherent states and measured using homodyne or heterodyne detection.

For DV-QKD, there are two main photon sources: weak coherent pulses (WCP) or polarization-entangled photon-pairs. Short attenuated pulses from laser diodes provide controlled weak coherent pulses that are needed to provide photon states for DV-QKD to enhance the security of these systems. Still, each pulse has a finite probability of containing more than a single photon. To avoid eavesdropping, decoy states have been created to reduce the likelihood of photon-number splitting attacks. One party randomly chooses between two intensities of coherent state signals, which is revealed to the other party, improving the tolerance to losses compared to the BB84 protocol that does not employ decoy states. This helps improving the transmitting distance and the key generation rate. Four laser diodes in a single transmitter are used to address the need for active polarization manipulation, allowing each laser to be identified with a single polarization state. By using a single laser diode coupled to four waveguides, the access to potential eavesdroppers is closed. Each waveguide is capable of a certain amount of polarization rotation and signals are then recombined into a single mode output with four possible polarization states.

Entanglement-based QKD require the generation of photons using polarization entangled photon pair sources. These sources are based on bulk-crystal, collinear, spontaneous parametric down conversion (SPDC), either periodically-poled potassium titanyl phospate (PPKTP) or single domain crystals such as beta barium oxide (BBO). SPDC is a non-linear process where a photon spontaneously splits into two other photon of lower energies. The pair pf photons are then distributed through a free space link to both Alice and Bob [11].

In order to assess the best QKD terminal for space, a trade-off between both sources has to be performed, taking into account certain aspects such as:

Quantum communication terminal physical features which assess the SwaP (size, weight and power consumption), the terminal performance based on the requirements to perform at a certain link distance, the capability to achieve the expected results, allow quantum link experiments that have a potencial for comercial interest and provide a classical optical communication link between the terminal and the base station. Other issues such as the development and the terminal costs, and the growth potential considering the improvement of possible applications such as to grow in link capacity are also of relevance.

Taking into account these aspects, in general, the EPS terminal is larger and heavier than the SPS terminal and also consumes more power. However, the range of possible experiments and their scientific impact is much higher using an EPS terminal than using a SPS terminal.

Entanglement-based secure QKD has been achieved over a physical distance of 1120 km at the Micius satellite experiments between two cities in China. Both ground stations were equipped with a 1.2 m diameter telescope. The satellite is equiped with a entanglement photon source that weights 23.8 Kg. A KTiOPO crystal inside a Sagnac interferometer is pumped by a continuous wave laser with a wavelength centered at 405 nm and a linewidth of 160 MHz, and generates polarization entangled photon pairs at 810 nm. The entangled photons are then guided by two single mode fibers to two transmitters which have a near-diffraction-limited far-field divergence of about 10 μrad. With a pump power of 30 mW the source is able to distribute up to 5.910^6 entangled photon pairs per second. The photons are then sent to two optical ground stations [12]. In figure 3.14 we can see the scheme of the entangled photon pair-source used in the Micius satellite experiments.

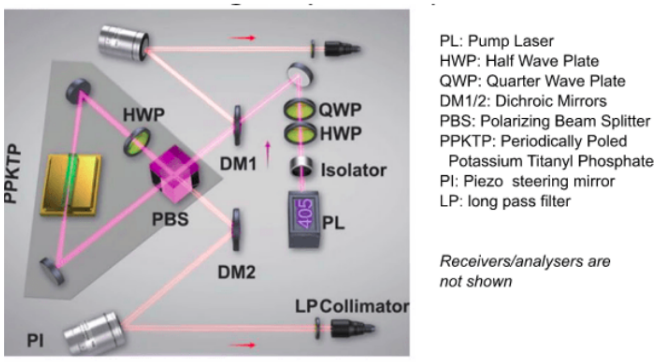

Fig. 10. A polarization entangled photon pair-source using PPKTP in a Sagnac loop arrangement. Used by the Micius Satellite double-downlink demonstrations [12]

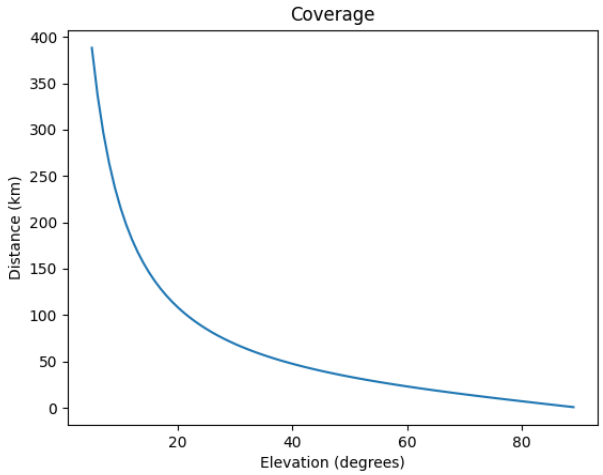

Fig. 12. Distance covered by a HAP at 20 km altitude for different elevation angles

IX. Results

A. Coverage Area

The two parameters that affect the satellite and HAP footprint on Earth are the height at which they are orbiting and the elevation angle which is the angle of the satellite/HAP in relation to a certain point on Earth. The smaller the elevation angle, the bigger is the area covered on Earth but the distance traveled is also longer which means that the signal will be more affected by the turbulence and other characteristics that will make the signal received at the detector have bigger losses. Also the elevation angle can not be too small because it will be affected by building when arriving at the Earth surface. In order to achieve the best relation between attenuation and covered area a good choice of the elevation angle is necessary. In the following figure we see different coverage areas (maximum distance between two points on the Earth surface) for a satellite at 500 km altitude and for a HAP at 20 km altitude, but for different elevation angles:

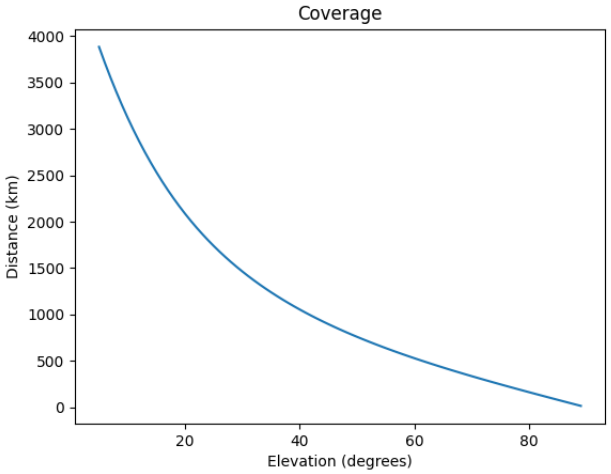

Fig. 11. Distance covered by a LEO at 500km altitude for different elevation angles

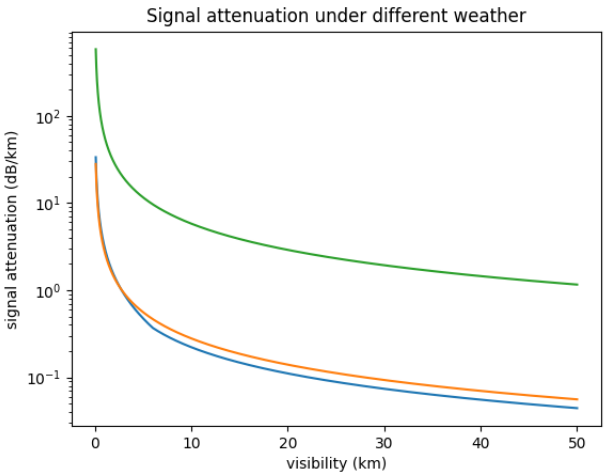

Fig. 13. Green: Snow; Red: Rain; Blue: Fog

B. Link Budget

In figure 13 we can see how the different type of weather affects the signal being transmitted:

Rain and fog have similar effects on the signal transmission whereas snow severely affects the signal, specially if the visibility is low. This means that with wild weather conditions it is almost impossible to transmit an optical signal through free space since the losses will be too high.

In the following table we simulate the values for certain parameters to obtain the link budget for a HAP at 20 km altitude and for a LEO satellite at 500 km altitude

Parameter	HAP	LEO satellite
Wavelength	850 nm	850 nm
Fried Parameter	0.2 m	0.2 m
Transmitter Aperture Size	0.1 m	0.1 m
Receiver Aperture Size	0.4 m	0.4 m
Altitude	20 km	500 km
Elevation Angle	5 to 90	5 to 90
Weather Altitude (Fog/Rain/Snow)	5 km	5 km
Rayleigh Losses (L_{atm})	3 dB	3 dB
Losses due to optical components (L_{opt})	6 dB	6 dB
T_t / T_p / T_r	0.8	0.8
BER	10^{-9}	10^{-9}
Power Required	-66 dB	-66 dB

Table 9.1: Link Budget Parameters

For the previous parameters the channel losses, with weather conditions not included) for a HAP at 20 km altitude with different elevation angles varies in the following way:

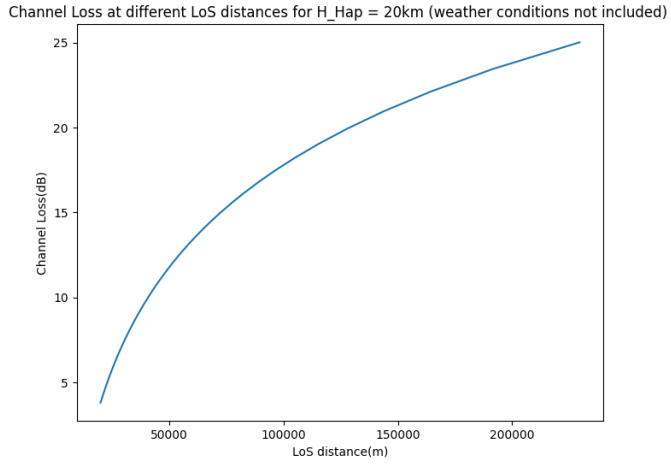

Fig. 14.

Now with the same parameters but for a LEO satellite orbiting at 500 km altitude for different elevation angles and not accounting for the atmospheric losses, the channel losses vary as pictured in figure 15.

As we can see from the graphics, the channel losses, non related with the atmospheric conditions, for a LEO satellite at 500 km altitude can go from as low as 30 dB for the highest elevation angle to around 55 dB for the lowest elevation angle, and for a HAP they can go as low as 12 dB for the highest elevation angle to around 25 dB at the lowest elevation angle.

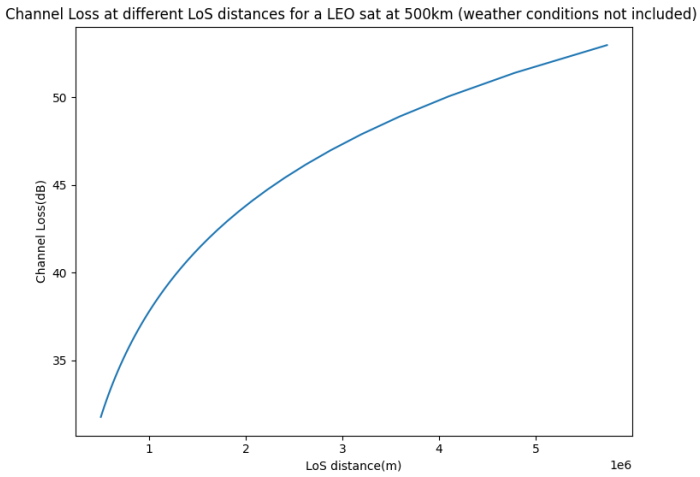

Fig. 15.

C. Pointing System

The percentage of hits by the beam on the receiver depends on several parameters such as: the beam divergence angle, which makes the diameter of the beam at the receiver increase with the distance, the gimbal error, which makes the centroid of the beam deviate from its original path, and the size of the receiver. Its possible to make a study about the percentage of hits versus no hits taking into account the previous parameters. In the following graph we can see the percentage of hits for a sample of 200 possible gimbal errors, for a 1 m receiver sizes and at different elevation angles (distances) for a HAP at 20 km altitude.

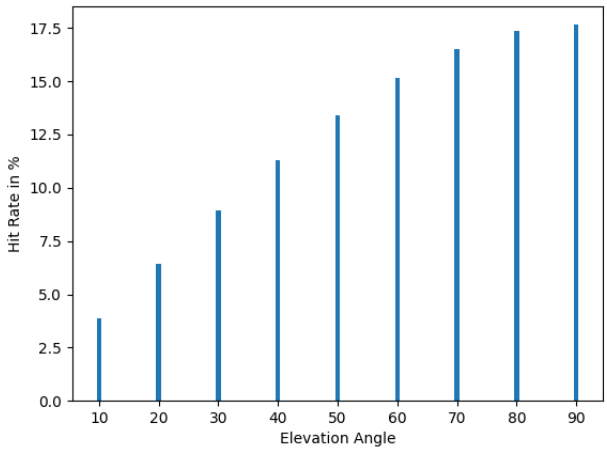

Fig. 16. Hit rate for a HAP at 20 km altitude and a 1 m aperture receiver

From the previous graphic we can see that the hit rate is much bigger for lower distances between the transmitter and the receiver. It has the same Hit rate for the last two distances due to the fact that the sample used for the gimbal error is not big enough to differentiate those two distances. We can now increase the size of the receiver to 2 m so that we can see the differences in the hit rate.

From figure 17 we can see that the size of the receiver dramatically increases the hit rate for a HAP at 20 km. In

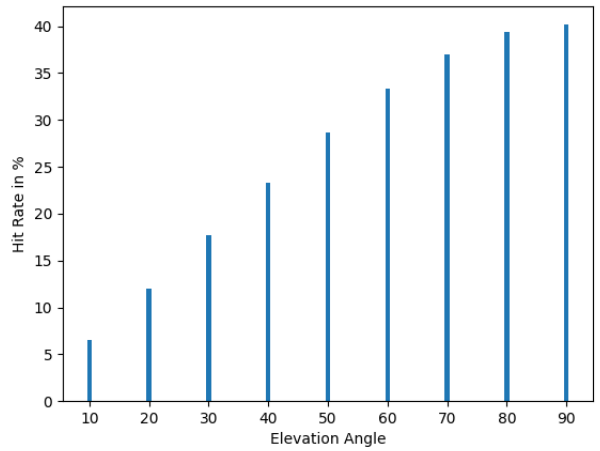

Fig. 17. Hit rate for a HAP at 20 km altitude and a 2 m aperture receiver

the next tables we will see how the same parameters affect a LEO satellite at 500 km altitude and if the parameters also have significant impact on the hit rate. The following graphic shows the hit rate for a LEO satellite at 500 km with a 1 m aperture receiver and a sample for the gimbal error of 10.000 different angles.

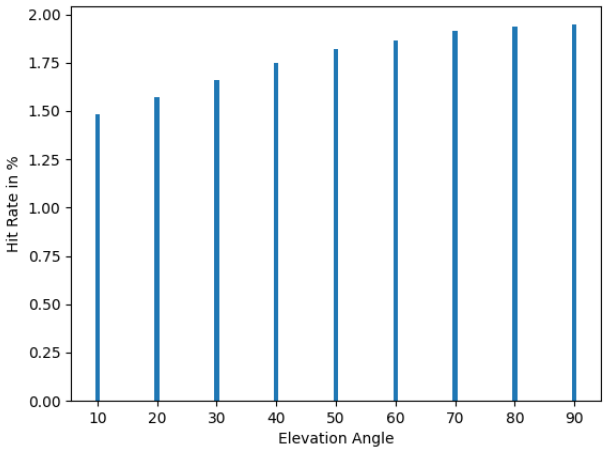

Fig. 18. Hit rate for a LEO at 500 km altitude and a 1 m aperture receiver

From figure 19 we see that with this gimbal error for a LEO satellite at 500 km, the hit rate is very low. This means that for the slightest movement of the gimbal, the laser will most likely miss the receiver. Now with the same parameters but for a 2 m receiver.

X. Conclusions

In this thesis the characteristics and properties of free space optical communications were studied along with the main challenges of having a QKD system on a LEO satellite or on a HAP in space, regarding the SWAP (size, weight and power) of a possible payload, the atmospheric turbulence that deviates the beam from its original path, the atmospheric conditions that affect the availability and the power of the signal received, the possible area covered by these two systems, and the need for an accurate acquisition, tracking and pointing system.

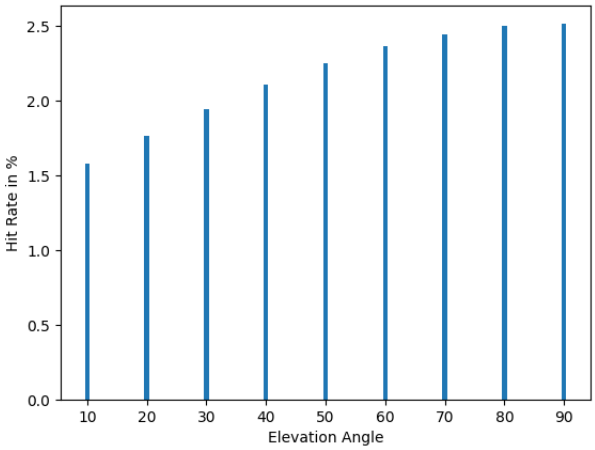

Fig. 19. Hit rate for a LEO at 500 km altitude and a 2 m aperture receiver

These while comparing both LEO satellites and HAPs. LEO satellites and HAPs have different purposes and so different characteristics. We concluded that the limitations regarding QKD in space can be overcome and using a payload on a HAP is a very promising alternative to LEO satellites.

XI. Bibliography

[1] Y. Chu, R. Donaldson, R. Kumar, and D. Grace. Feasibility of quantum key distribution from highaltitude platforms.Quantum Science and Technology, 2021.

[2] S. Cakaj, B. Kamo, A. Lala, and A. Rakipi. The coverage analysis for low earth orbiting satellites atlow elevation.International Journal of Advanced Computer Science and Applications, 5(6), 2014.

[3] J. Guimar aes, M. J. Martins, and A. Baptista. Optical inter-satellite links: Applications in defense.PROELIUM, 7:361–379, 2016.

[4] W.-C. Wang. Optical detectors.Department of Power Mechanical Engineering, National Tsing HuaUniversity. https://depts. washington. edu/mictech/optics/me557/detector. pdf, 12, 2011.

[5] O.˘Cierny. Precision closed-loop laser pointing system for the nanosatellite optical downlink exper-iment, 2017.

[6] M. Pfennigbauer, M. Aspelmeyer, W. Leeb, G. Baister, T. Dreischer, T. Jennewein, G. Neckamm,J. Perdigues, H. Weinfurter, and A. Zeilinger. Satellite-based quantum communication terminalemploying state-of-the-art technology.Journal of Optical Networking, 4(9):549–560, 2005.

[7] Y. Chu, R. Donaldson, R. Kumar, and D. Grace. Feasibility of quantum key distribution from highaltitude platforms.Quantum Science and Technology, 2021.

[8] E. Kerstel, A. Gardelein, M. Barthelemy, M. Fink, S. K. Joshi, and R. Ursin. Nanobob: a cubesatmission concept for quantum communication experiments in an uplink configuration.EPJ QuantumTechnology, 5(1):6, 2018.

[9] K. Cahoy, P. Grenfell, A. Crews, M. Long, P. Serra, A. Nguyen, R. Fitzgerald, C. Haughwout, R. Diez,A. Aguilar, et al. The cubesat laser infrared crosslink mission (click). InInternational Conferenceon Space Optics—ICSO 2018, vol-

ume 11180, page 111800Y. International Society for Optics andPhotonics, 2019.

[10] D. Bouwmeester and A. Zeilinger. The physics of quantum information: basic concepts. InThephysics of quantum information, pages 1–14. Springer, 2000.

[11] O. Lee and T. Vergoossen. An updated analysis of satellite quantum-key distribution missions.arXiv preprint arXiv:1909.13061, 2019.

[12] P. Jianwei. Progress of the quantum experiment science satellite (quess) micius project. , 38(5):604–609, 2018.